Copyright Notice

(Article begins on next page)

Operational Regime of Symbol-by-Symbol Phase Noise Estimation for POLMUX 16-QAM

Fangrong Peng[(1)], Henk Wymeersch[(1)], A. Serdar Tan[(1)], Martin Sjödin[(2)], Pontus Johannisson[(2)], Erik Agrell[(1)], Peter Andrekson[(2)], Magnus Karlsson[(2)]

[(1)] Communication Systems Group, Department of Signals and Systems, Chalmers University of Technology, SE-412 96 Göteborg, Sweden ✉ henkw@chalmers.se
[(2)] Photonics Laboratory, Department of Microtechnology and Nanoscience, Chalmers University of Technology, SE-412 96 Göteborg, Sweden

Abstract *A symbol-by-symbol phase noise estimation algorithm for polarization-multiplexed 16-QAM is evaluated. We found that it can cope with laser linewidths of up to 2.2 MHz in high SNR regimes, at 112 Gbit/s.*

Introduction

Coherent 16-QAM polarization multiplexed (POLMUX) transmission has the potential to double throughput compared to QPSK-POLMUX, but is more sensitive to impairments in the transmission link. In particular, phase noise caused by the non-zero linewidth of lasers is an impairment that needs to be compensated for prior to data detection. Phase noise is characterized by the product $\Delta_\nu T$, where Δ_ν is the sum of the linewidths of the signal and local oscillator lasers, and $1/T$ is the baud rate. Feedback phase noise estimation using a phase-locked loop can only cope with small $\Delta_\nu T$, while feed-forward (FF) phase noise estimation is promising for larger $\Delta_\nu T$[1,2]. FF estimation is based on block processing, considering the phase to be approximately constant over the duration of a block. As the block size decreases, faster adaptation is possible but with degraded estimation performance[3]. For QPSK, values of $\Delta_\nu T \approx 10^{-3}$ can be tolerated with negligible loss under FF estimation[2], but for 16-QAM, the reduced angular separation and the presence of multiple amplitude levels reduces the phase noise tolerance. Symbol-by-symbol phase estimators (SBSPE) are a potential way to cope with larger values of $\Delta_\nu T$. They can be seen as a special case of block-based estimators[3,5], and have also received considerable interest on their own[4,6].

In this paper, we (i) provide the first explicit derivation of an SBSPE; (ii) analyze the error probability of the ring detector[3–6]; (iii) discuss the SNR and $\Delta_\nu T$ regime in which SBSPE can operate reliably, confirming previous experimental findings[4]; (iv) develop a novel algorithm to combine estimates from both polarizations. Through Monte Carlo simulations, we demonstrate the superior performance of the SBSPE, compared to state-of-the-art block-based estimators[4].

Observation Model

The baud-rate samples, after timing recovery and compensation for polarization changes, PMD, and CD, can be expressed as

$$\mathbf{r}_k = \begin{bmatrix} a_k^{(\mathrm{X})} e^{j\theta_k} \\ a_k^{(\mathrm{Y})} e^{j\phi + j\theta_k} \end{bmatrix} + \mathbf{n}_k, \qquad (1)$$

where $a_k^{(i)}$ is the kth 16-QAM symbol on polarization $i \in \{\mathrm{X}, \mathrm{Y}\}$, $\mathbf{n}_k$ is modeled as independent and identically distributed zero-mean complex Gaussian noise with variance σ^2 per real dimension per polarization, ϕ is a phase offset between X and Y polarization, and θ_k is the phase noise. For notational convenience, we will set $\phi = 0$, as this parameter can be estimated accurately from a long block of observations, and focus on a single polarization so that we can drop the superscripts X and Y, and write r_k for the scalar observation at time k. The SNR is defined as $E_\mathrm{s}/(2\sigma^2)$, where E_s is the average energy per 16-QAM symbol per polarization.

A conventional FF estimator operates as follows. First, the observation is broken into blocks of length M, with the phase estimate in the kth block given by the Viterbi&Viterbi estimator[7]

$$\hat{\theta}_k^{\mathrm{r}} = \frac{1}{4} \measuredangle \left(\sum_{l=s_k}^{s_k+M-1} r_l^4 \right), \qquad (2)$$

where $\measuredangle(\cdot)$ denotes the phase and s_k is the index of the first symbol in the kth block. Note that the phase estimates will fall in the range $[0, \pi/2)$. Hence, the estimates must unwrapped and may be low-pass filtered. Unwrapping[1] is denoted as $\hat{\theta}_k^{\mathrm{u}} = \mathrm{U}(\hat{\theta}_k^{\mathrm{r}}, \hat{\theta}_{k-1}^{\mathrm{u}})$, in which $\hat{\theta}_{k-1}^{\mathrm{u}}$ serves as the ref-

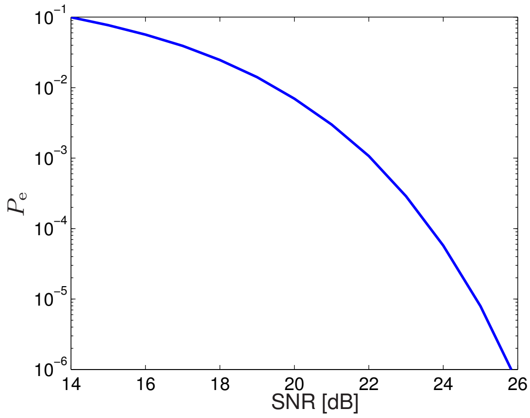

Fig. 1: Error probability of the ring detector from (3).

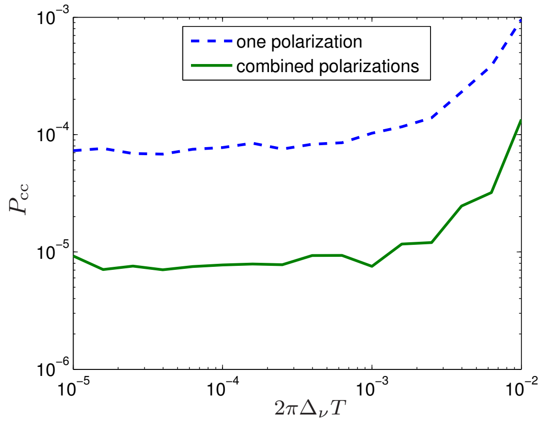

Fig. 2: Probability of cycle slips for different laser linewidths, using one and two polarizations.

erence phase for $\hat{\theta}^\text{u}_k$. The superscripts $\cdot^\text{r}$ and $\cdot^\text{u}$ refer to *raw* and *unwrapped* phase estimates, respectively. An SBSPE version of (2) corresponds to $M = 1$.

Symbol by Symbol Phase Estimator

The estimator (2) is based on the four-fold rotational symmetry of 16-QAM: symbols lie on 3 distinct rings, with $\measuredangle a_k^4 = \pi$ for symbols on the outer or inner ring, while $\measuredangle a_k^4 = \pm 4 \arctan(1/3)$ for symbols on the middle ring. For the effect of these latter symbols to be averaged out in (2), we require $M \gg 1$. In contrast, for QPSK $\measuredangle a_k^4 = \pi$ for *all* symbols, so that with $M = 1$, we can still have a reliable phase estimate under QPSK transmission. Hence, to circumvent this averaging in 16-QAM, an SBSPE must first detect on which ring the transmitted symbol lies.

Ring discrimination: Introducing $\rho_k = |r_k|^2$, for medium-to-high SNR, we can model $\rho_k \sim \mathcal{N}(\mu_{R,\sigma^2}, V_{R,\sigma^2})$, where R is the radius of the circle on which the kth transmitted symbol lies. We find that $\mu_{R,\sigma^2} = R^2 + 2\sigma^2$ and $V_{R,\sigma^2} = 4\sigma^4 + 4R^2\sigma^2$. The optimal, maximum a posteriori estimate of the ring, given the observation ρ_k, is then

$$\hat{R}_k = \arg\max_R \left\{ \log \frac{p(R)}{V_{R,\sigma^2}} - \frac{\left(\rho_k - \mu_{R,\sigma^2}\right)^2}{2V_{R,\sigma^2}} \right\}, \tag{3}$$

where the maximization occurs over $R \in \{R_\text{i}, R_\text{m}, R_\text{o}\}$, for the inner, middle, and outer ring, respectively, with $p(R_\text{i}) = p(R_\text{o}) = p(R_\text{m})/2 = 1/4$.

Phase estimation: Once the ring has been determined, the phase can be estimated as follows. We denote by $\hat{\theta}^\text{r}_k = 1/4 \measuredangle r_k^4$. When $\hat{R}_k \in \{R_\text{i}, R_\text{o}\}$ we find $\hat{\theta}^\text{u}_k = \text{U}(\hat{\theta}^\text{r}_k, \hat{\theta}^\text{u}_{k-1})$. On the other hand, when $\hat{R}_k = R_\text{m}$ we have two potential phase estimates (say, $\hat{\theta}^{\text{r},1}_k$ and $\hat{\theta}^{\text{r},2}_k$) and choose the one that is most likely, assuming small phase noise steps are more likely than large ones: introducing $\alpha_k = \text{U}(\hat{\theta}^{\text{r},1}_k, \hat{\theta}^\text{u}_{k-1})$ and $\beta_k = \text{U}(\hat{\theta}^{\text{r},2}_k, \hat{\theta}^\text{u}_{k-1})$, we find that

$$\hat{\theta}^\text{u}_k = \arg\min_{\alpha_k, \beta_k} \left(|\alpha_k - \hat{\theta}^\text{u}_{k-1}|, |\beta_k - \hat{\theta}^\text{u}_{k-1}| \right). \tag{4}$$

Extension to POLMUX: On each polarization, we get an independent estimate of the *common* phase θ_k. The quality of the estimate depends on the ring on which the transmitted symbol lies. There are four possible cases: (i) $\hat{R}^{(\text{X})}_k = \hat{R}^{(\text{Y})}_k \in \{R_\text{i}, R_\text{o}\}$ (ii) $\hat{R}^{(\text{X})}_k = R_\text{i}$ and $\hat{R}^{(\text{Y})}_k = R_\text{o}$ (or vice versa); (iii) $\hat{R}^{(\text{X})}_k \in \{R_\text{i}, R_\text{o}\}$ and $\hat{R}^{(\text{Y})}_k = R_\text{m}$ (or vice versa); and (iv) $\hat{R}^{(\text{X})}_k = \hat{R}^{(\text{Y})}_k = R_\text{m}$.

In cases (i)-(ii), the variance of the estimates is $\sigma^2/(\hat{R}^{(\text{X})}_k)^2$ and $\sigma^2/(\hat{R}^{(\text{Y})}_k)^2$, respectively. We can combine these estimates by weighing them with their precisions, as follows. Letting $\gamma_k = \text{U}(\hat{\theta}^{\text{r},(\text{X})}_k, \hat{\theta}^{\text{r},(\text{Y})}_k)$, we can find a joint estimate of θ_k as

$$\hat{\theta}^\text{r}_k = \frac{(\hat{R}^{(\text{X})}_k)^2 \gamma_k + (\hat{R}^{(\text{Y})}_k)^2 \hat{\theta}^{\text{r},(\text{Y})}}{(\hat{R}^{(\text{X})}_k)^2 + (\hat{R}^{(\text{Y})}_k)^2}. \tag{5}$$

In case (iii), $\hat{R}^{(\text{X})}_k$ can serve as a phase reference for the Y polarization, i.e., by replacing $\hat{\theta}^\text{u}_{k-1}$ by $\hat{\theta}^{\text{r},(\text{X})}$ in (4), after which we apply (5) with appropriate weighting. In case (iv), we apply (4) to the X and Y polarization, followed by (5) with weigths $1/2$.

Numerical Results

We have investigated the performance of the SBSPE for a Wiener noise phase model, with variance $\sigma_\theta^2 = 2\pi\Delta_\nu T$. The performance of a phase noise estimator is characterized through two fig-

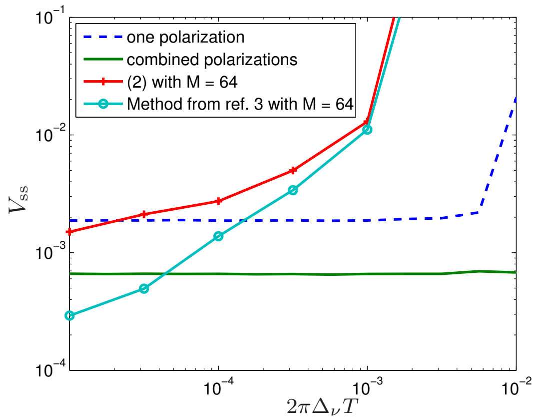

Fig. 3: Steady-state error variance for different laser linewidths, using one and two polarizations.

ures of merit: the probability of cycle slips and the steady-state variance of the estimation error in between cycle slips. Cycle slips are highly non-linear events that occur during the unwrapping stage. They cause potentially catastrophic $\pi/2$ jumps that can be averted by employing differential modulation[1]. On the other hand, the steady-state variance determines the performance of the subsequent data detection.

Cycle slips: Cycle slips are likely to occur when the algorithm (3) fails. Errors in the ring discrimination are dominated by mistaking R_{m} and R_{o} and can be determined analytically. The computed error probability (P_{e}) is shown in Fig. 1. Observe that relatively large SNR values are required to keep P_{e} low, a fact that was also observed empirically[4]. Also note that the SNR required for a nominal BER of 10^{-3} is around 19 dB, where P_{e} is over 1%. In the subsequent results, we set the SNR to 24 dB, similar to previous findings[4], corresponding to $P_{\mathrm{e}} \approx 5 \times 10^{-5}$ and a BER of 10^{-7}. Now, we consider the probability of cycle slips (P_{cc}) as a function of σ_θ^2, where the phase is estimated separately per polarization or jointly (using (5)). Cycle slips probabilities are estimated based on long transmissions, where the number of cycle slips are counted and then divided by the transmission length (in symbols). The results, shown in Fig. 2, indicate that cycle slips start occuring more often for $\sigma_\theta^2 > 10^{-3}$, corresponding to a laser linewidth of up to 2.2 MHz at 112 Gbit/s. Furthermore, fusing information from both polarization reduces the probability of cycle slips by about an order of magnitude.

Variance of the estimation error: In between cycle slips, the performance of the SBSPE is characterized by the steady-state variance $V_{\mathrm{ss}} = \mathbb{E}\left\{(\theta_k - \hat{\theta}_k^{\mathrm{u}})^2\right\}$, where $\mathbb{E}\{\cdot\}$ denotes the expectation operator. The results, shown in Fig. 3, are similar to Fig. 2, in that the performance is fairly independent of σ_θ^2 up to $\sigma_\theta^2 > 10^{-3}$, above which V_{ss} increases rapidly. For 112 Gbit/s communication, laser linewidths up to 2.2 MHz can be tolerated. It should be noted that, contrary to block-based estimators[5] the proposed SBSPE leads to nearly independent phase estimates, and can thus be combined with phase filtering techniques[1], to reduce V_{ss} with multiple orders of magnitude. We have also included the performance of the estimator 2 for $M = 64$, and the estimator from[3] with $M = 64$. Observe that the proposed SBSE can tolerate about one order of magnitude more laser linewidth.

Conclusions

In this paper, we have described and analyzed a phase estimator for POLMUX 16-QAM that operates on one symbol at a time, thus allowing tracking of rapidly varying phases. We have provided an analysis of this estimator, corroborating experimental findings from other authors. We show that even though high SNR is required for the estimator to work properly, it is robust for laser linewidths of up to 2.2 MHz at 112 Gbit/s.

Acknowledgement

We like to acknowledge funding from the Swedish Strategic Research Foundation, SSF, as well as VINNOVA within the IKT grant.

References

1 E. Ip et al., JLT, **25**, 2675, (2007).
2 T. Pfau et al., JLT, **27**, 989, (2009).
3 M. Seimetz, OFC 2008, OTuM2 (2008).
4 H. Louchet et al., ECOC 2008, Tu.1.E.6 (2008).
5 I. Fatadin et al., PTL, **22** (2010).
6 F. Rice et al., DSP, **12**, 77, (2002).
7 A.J. Viterbi et al., IEEE Trans. Inform. Theory, **IT-29**, 543, (1983).